



City Research Online

City, University of London Institutional Repository

Citation: Reyes-Aldasoro, C. C., Björndahl, M. A., Ibrahim, J., Akerman, S. & Tozer, G. M. (2010). A scale-space tracing algorithm for analysis of tumour blood vessel morphology from transmitted light optical images. Poster presented at the 2010 NCRI Cancer Conference, 31-10-2010 - 03-11-2010, Liverpool, UK.

This is the published version of the paper.

This version of the publication may differ from the final published version.

Permanent repository link: <https://openaccess.city.ac.uk/id/eprint/5441/>

Link to published version:

Copyright: City Research Online aims to make research outputs of City, University of London available to a wider audience. Copyright and Moral Rights remain with the author(s) and/or copyright holders. URLs from City Research Online may be freely distributed and linked to.

Reuse: Copies of full items can be used for personal research or study, educational, or not-for-profit purposes without prior permission or charge. Provided that the authors, title and full bibliographic details are credited, a hyperlink and/or URL is given for the original metadata page and the content is not changed in any way.

City Research Online:

<http://openaccess.city.ac.uk/>

publications@city.ac.uk

A scale-space tracing algorithm for analysis of tumour blood vessel morphology from transmitted light optical images

Constantino Carlos Reyes-Aldasoro, Meit A. Björndahl, Jamila Ibrahim, Simon Akerman and Gillian M. Tozer
 Cancer Research UK Tumour Microcirculation Group, Department of Oncology, The University of Sheffield
 K Floor, Royal Hallamshire Hospital, Sheffield S10 2RX
<http://www.caiman.org.uk>
c.reyes@sheffield.ac.uk



Background

Limited contrast in optical images from intravital microscopy is problematic for analysing tumour vascular morphology. Moreover, in some cases, changes in vasculature are visible to a human observer but are not easy to quantify. We present 2 methodologies to quantify the characteristics of vasculature: first through measurements of the vessel morphology and second through the observation of its chromatic characteristics. We evaluated the methodologies on images from SW1222 human colorectal carcinoma cells transfected with angiopoietin **Ang-1** or **Ang-2** cDNA, or with an empty vector (**WT**) and implanted into **window chamber-bearing mice**. 464 transmitted light images (x10 objective) were acquired from 29 restrained mice (11 Ang-1, 12 Ang-2, 6 WT) in 2 regions of interest before and up to 24h [0, 2.5, 15, 30, 60, 180, 360, 1440 min] (Fig. 1) after treatment with 30 mg/kg of the vascular disrupting agent **combrestatin A-4-P (CA-4-P)** or saline.

How do we measure vascular changes with treatment?

Method 1 Morphology

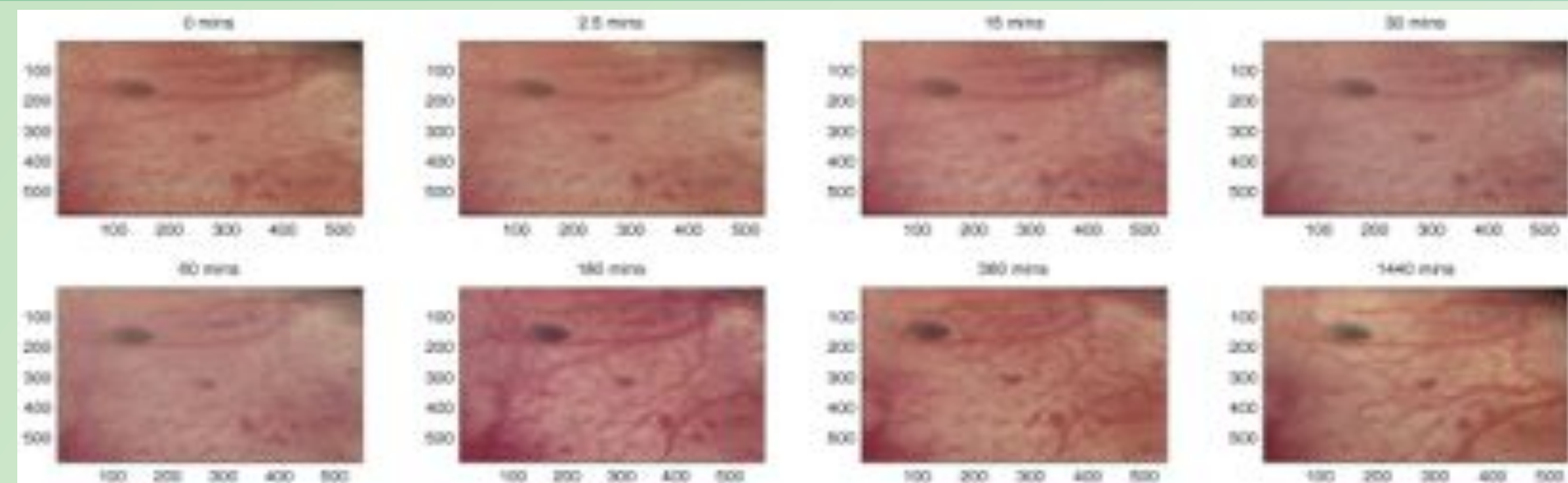


Fig. 1 Eight images of the vasculature in a dorsal window chamber as observed through intravital microscopy in a mouse treated with CA-4-P. Notice the colour variation and changes in vasculature with time.

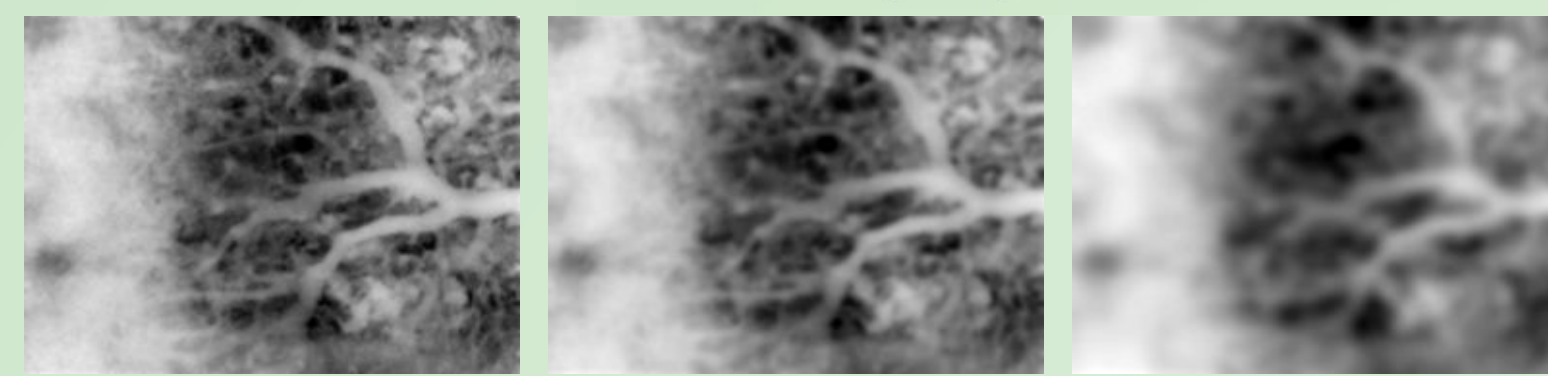
Method 2 Chromaticity



Vessel tracing used a **scale-space approach** (Lindeberg, 1998a; Lindeberg, 1998b) employing differences in intensity of transmitted light between the vessels and surrounding tissues. The centreline of vessels was detected as a **ridge** in a topographical analogy and successive levels of filtering provided different scales to detect sharp to diffuse ridges. Morphological parameters were measured from the traced images - average vessel length (AL) width (AW), and relative vascular area (RA).

Scale-space representation of a function $f(x,y)$ can be defined as the convolution with a Gaussian $g(x,y,t)$ where t corresponds to the width of the Gaussian. Then, the normalised first and second derivatives in x and y dimensions ($L_x, L_{xx}, L_{xy}, L_y, L_{yy}$), which form the **Hessian Matrix** \mathcal{H} , will highlight the rate of change of the intensities of the images. Regions of maxima and minima can be calculated when the derivatives reach zero. To obtain the centrelines of vessels, or ridges in a topological analogy, it is necessary to convert from the (x,y) coordinate system to a **local (p,q) system** aligned with the **eigendirections** of the Hessian Matrix, β corresponds to the angle of rotation of the coordinate system. The ridges at different scales constitute a **scale-space ridge surface** and are defined as the points of $(L_p, L_{pp}, L_q, L_{qq})$ that fulfil the conditions of maxima at every scale. Finally, the ridge surface needs to be simplified by selecting the points where the ridge surface has maximal values by a given norm. Thus, fine ridges are detected at fine scales whilst coarse ridges will have higher norm values at larger scales. The detected **scale-space ridges** can be ranked by the strength of the ridge, which indicates which ridges are better defined in the contrast between the ridge itself and the surrounding regions (Fig. 2).

$$L(x,y,t) = g(x,y,t) * f(x,y) = \frac{1}{(2\pi t)} e^{-(x^2+y^2)/(2t)} * f(x,y)$$



$$\mathcal{H} = \begin{bmatrix} \partial_x \partial_x f & \partial_x \partial_y f \\ \partial_x \partial_y f & \partial_y \partial_y f \end{bmatrix} = \begin{bmatrix} L_{xx} & L_{xy} \\ L_{xy} & L_{yy} \end{bmatrix}$$

$$L_p = \partial_p L = (\sin \beta \partial_x - \cos \beta \partial_y) L$$

$$L_q = \partial_q L = (\cos \beta \partial_x + \sin \beta \partial_y) L$$

$$\cos \beta_{(L_p, L_q)} = \sqrt{\frac{1}{1 + \frac{L_{xx} - L_{yy}}{(L_{xx} - L_{yy})^2 + 4L_{xy}^2}}}$$

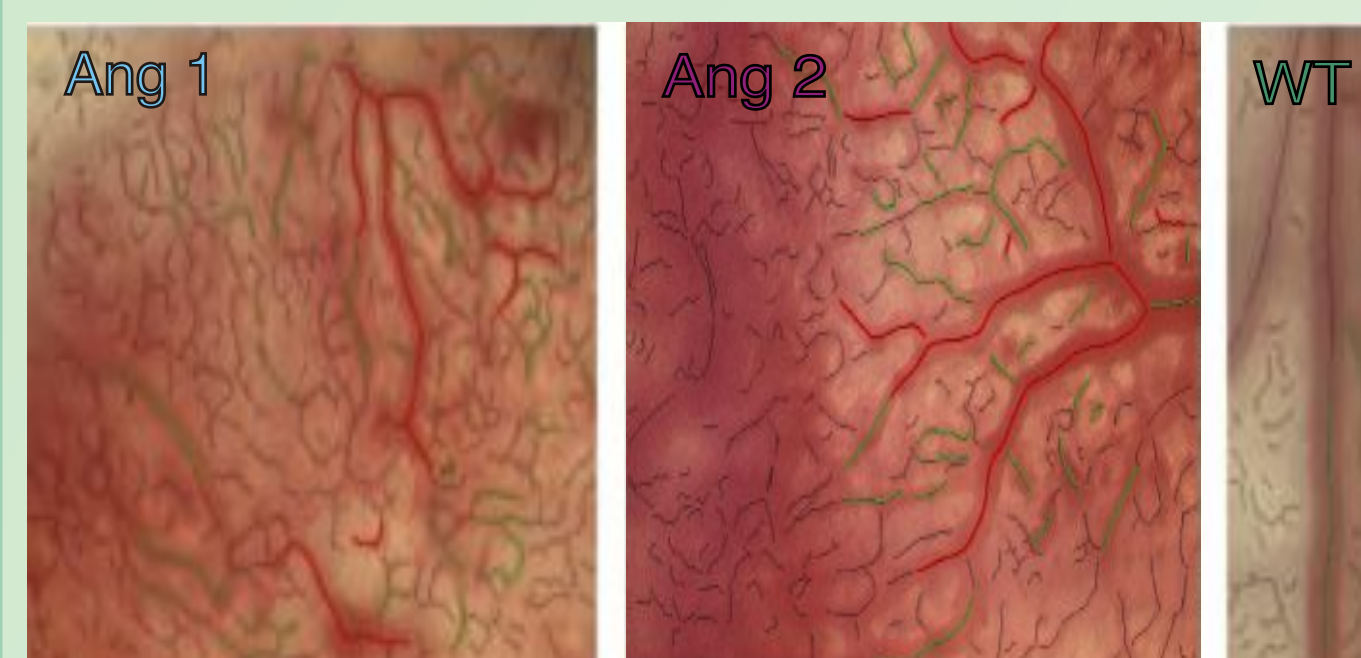
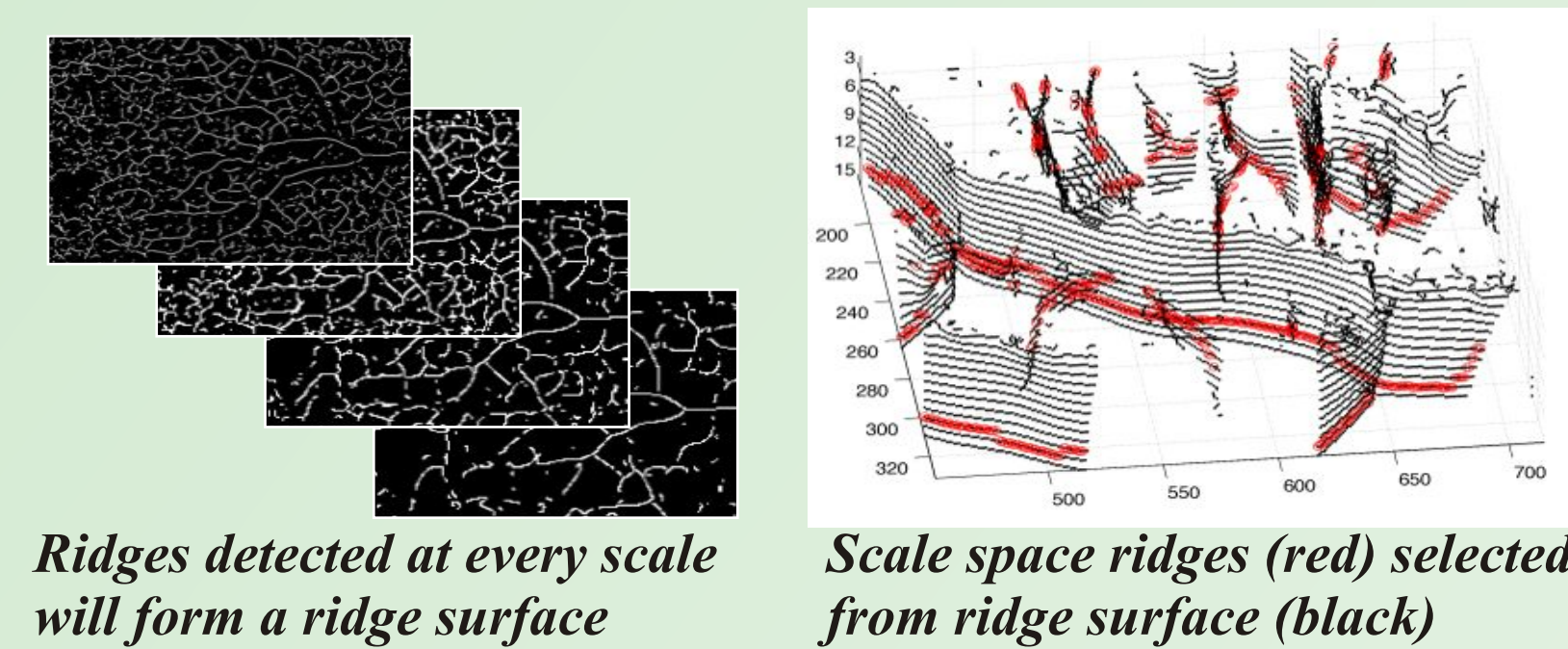
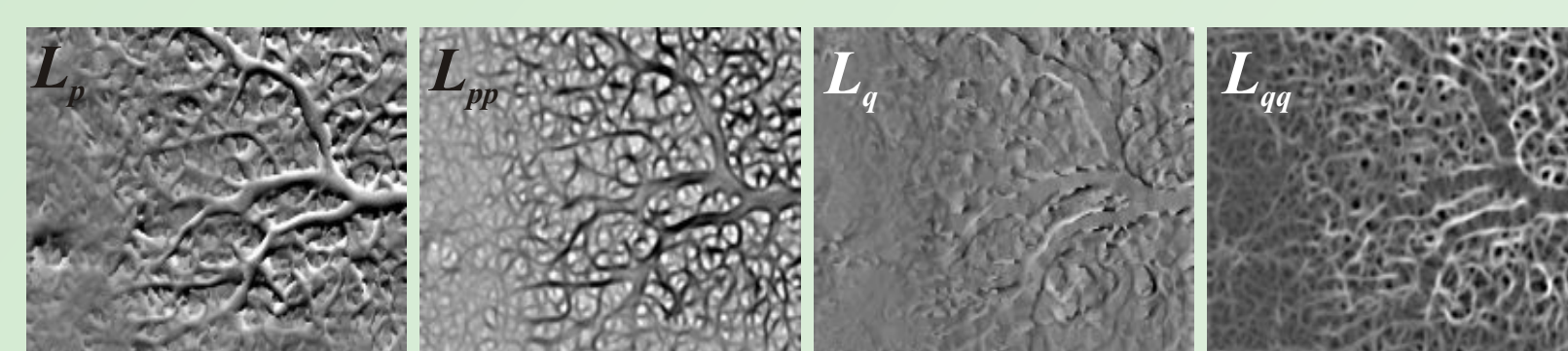


Fig. 2. Three examples of the vasculature tracing by scale-space. The algorithm detected vessels in an analogy to topological ridges at different scales, selected the optimal scale (i.e. related to the width of the vessel) and then ranked them according to the strength of the ridge (i.e. how well defined the ridge is). Ten strongest ridges are labelled in red, the next 40 in green and the rest in black.

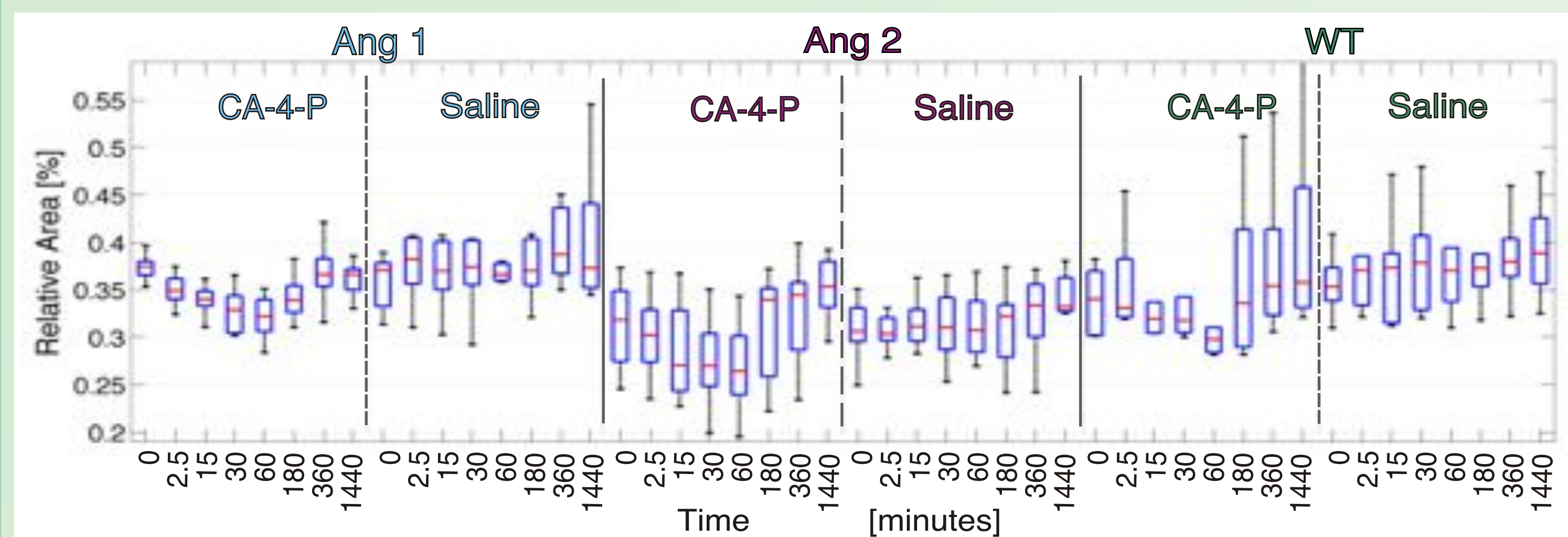


Fig. 3. Boxplots describing the morphological changes in tumour vasculature. The relative area covered by the vessels remains constant with saline treatment. However CA-4-P induces a decrease (vessels become thinner and shorter) up to one hour, after which it starts to recover. Notice the lower values of Ang-2 relative to Ang-1.

The **Hue, Saturation, Value** (HSV) colour model describes perceptual colour relationships related to the artistic ideas of hue, tint and shade and is better for discrimination of structures than the **Red, Green, Blue** (RGB) colour space (Reyes-Aldasoro 2010a). While hue is related to the wavelength or the **tint** of the image, saturation indicates the purity of a colour (**saturation = 1**) or how close to white or grey (**saturation = 0**) and thus devoid of colour. For this study we were interested in detecting if the images became **paler** with time and how this reflected in the saturation. The chromatic changes of the images can be visualised from the 2D / 3D HSV histograms m_{HS} , m_{HSV} (Figs. 4,5) and a **saturation balance** was calculated as the ratio between the number of pixels in the 50% least saturated region to the total number of pixels.

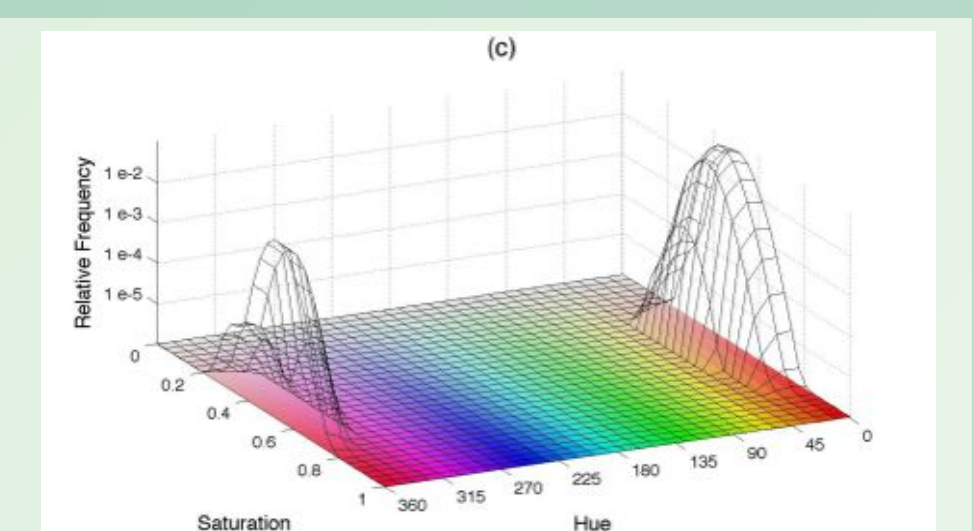


Fig. 4. The 2D m_{HS} histogram where peaks denote the occurrence of pixels of certain hues/saturations. Most pixels are in the warm regions of red, orange and brown.

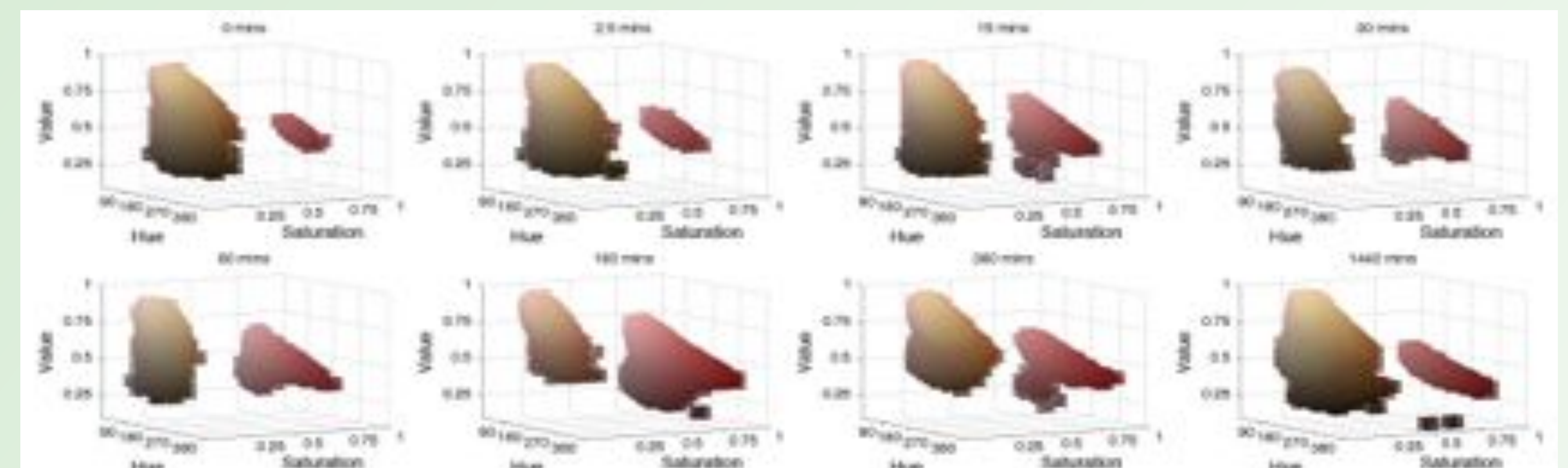


Fig. 5. The 3D m_{HSV} histograms corresponding to the images of Fig. 1. Clouds of points describe pixels according to hues, saturation and value. Notice the changes in the clouds; the red cloud (right hand side) grows and then decreases in size. Both clouds increase their pale/bright region, which later on decreases.

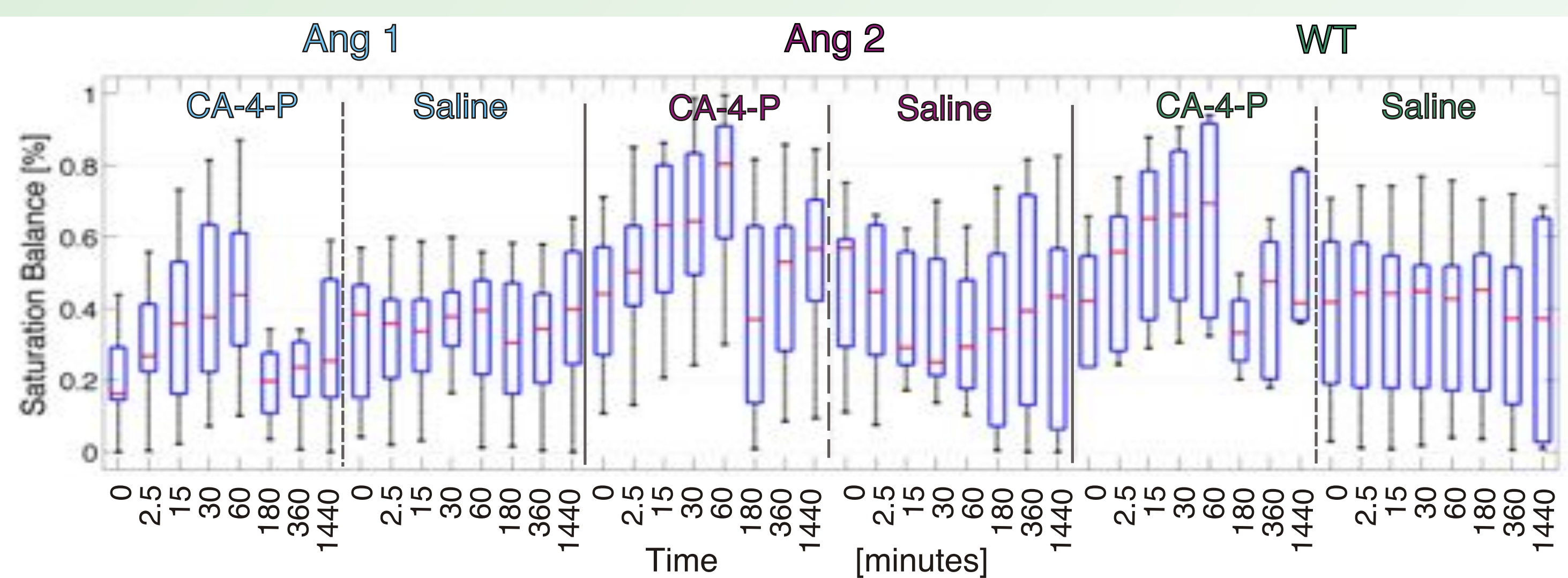


Fig. 6. Boxplots describing the chromatic changes in saturation balance. While saturation balance remains constant with saline treatment, CA-4-P induces an increase (images become paler, whiter) up to one hour, after which saturation returns to previous levels.

Results

- (1) Decrease in Relative Area:** the algorithm successfully identified the majority of tumour microvessels. CA4P-treated tumours showed a decrease in average length and width of detected vessels (box plots not shown) and the combined relative area covered by the vessels up to 1-3h, with recovery by 24h. Saline had no effect. Ang-2 over-expressing tumours had lower values of length, width and relative area than Ang-1 and wild-type tumours. Ang-1 tumours were similar to the WT except that average length was longer.
- (2) Increase in saturation balance:** Chromaticity analysis showed a trend in the CA-4-P treated images to increase the ratio of pixels with low saturation (i.e. closer to white) relative to total pixels during the first hour after treatment, later to return to initial levels. Also, the hues shifted from brown-orange to red-purple in the same time as the saturation (box plots not shown) with a similar recovery.

Conclusions

The increase in saturation balance (Fig. 6) and the decrease in relative vascular area (Fig. 3) may be due to the changes in oxygenation in the tissue following CA-4-P. Over-expression of Ang-2 resulted in excessively branching and narrow vessels, indicative of a high vascular resistance, potentially influencing response to therapy. Although no differential response to CA-4-P was found between the angiopoietins, investigation of functional vascular parameters is needed to confirm this conclusion.

We thank Prof. Barbara Pedley, University College London, for the untransfected SW1222 cells.

References:

Lindeberg, T., 1998a. Edge and ridge detection with automatic scale selection. *Int J Computer Vision*. 30, 117-154.
 Lindeberg, T., 1998b. Feature detection with automatic scale selection. *Int J Computer Vision*. 30, 79-116.
 Reyes-Aldasoro, C. C., et al., 2010a. An automatic segmentation algorithm for the morphological analysis of microvessels in immunostained histological tumour sections. *J Microscopy*. in press
 Reyes-Aldasoro, C. C., et al., 2010b. CAIMAN: An online algorithm repository for Cancer Image Analysis. *Comput. Meth. Prog. Bio*. in press.

This work was funded by

